ELSEVIER

Comput. Methods Appl. Mech. Engrg. 190 (2000) 25–34

Computer methods in applied mechanics and engineering

www.elsevier.com/locate/cma

# The laser displacement measurement with feedback control in a magnetic levitation and suspension system

Chern-Sheng Lin [a,*], Yun-Long Lay [b], Pei-Wen Chen [c], Young-Jou Jain [a], Shiaw-Wu Chen [a]

[a] *Department of Automatic Control Engineering, Feng Chia University. Taichung, Taiwan, ROC*
[b] *Department of Electronics Engineering, National Chin-Yi Institute of Technology, Taichung, Taiwan, ROC*
[c] *Department of Electronics Engineering, Chien Huo Junior College, ChungHua, Taiwan, ROC*

Received 15 April 1999

**Abstract**

In this study, we used a laser displacement sensor, which the resolution was precise over 2 μm and capable of measuring infinitesimal displacement rapidly for magnetic levitation and suspension equipment. A feedback control was applied in this system, which required quick response to voltage variations. We also derived the equations of motion to determine the stability limits and compared our calculations with the experimental results. From the experimental results, this mag-lev system, with special optical sensors and feedback circuits, is able to dynamically adjust unstable levitation positions. 

*Keywords:* Laser displacement sensor; Magnetic levitation; Suspension; Feedback control

## 1. Introduction

Precision measurement always plays an important role in the field of auto-control. Electro-optics measurement is more exact and accurate, and has the advantages of non-contact and real-time, therefore this is the preferred method measurement and control whenever applicable. The advantages of an optical sensor [1–3] in the electric-mechanical field also lies in the simplicity of construction, precision and high frequency response. Here we employed a special feedback control with laser displacement measurement feedback to improve the conventional PID control method in a magnetic levitation and suspension system (Fig. 1). Using three laser displacement sensors, we acquired a gap value, between the core of an E-type and armature of an I-type, and converted it to a voltage value through a coil on the core. Although the laser displacement sensor can measure the gap value rapidly and accurately, in practical experiments, we must solve many problems such as program design, signal transmittance and noise disturbances, etc.

In the laser displacement sensor [4,5], a diode laser was focused onto the actuator of the mag-lev system being measured using an objective lens in order to provide a small measurement spot. The size and intensity of the optical spot onto the detector is usually not critical, since the detector will sense the centroid of the spot. A wavelength selective filter in front of the detector was installed to isolate the ambient light and increase the signal-to-noise ratio. Since the focused laser beam is small, the resolution, acquisition and measurement range is quite large. The calibration procedures for the laser displacement in combination with the mag-lev system, can correct the initial nonlinearities by tabulating corrections.

* Corresponding author.

0045-7825/00/$ - see front matter 
PII: S0045-7825(00)00186-9

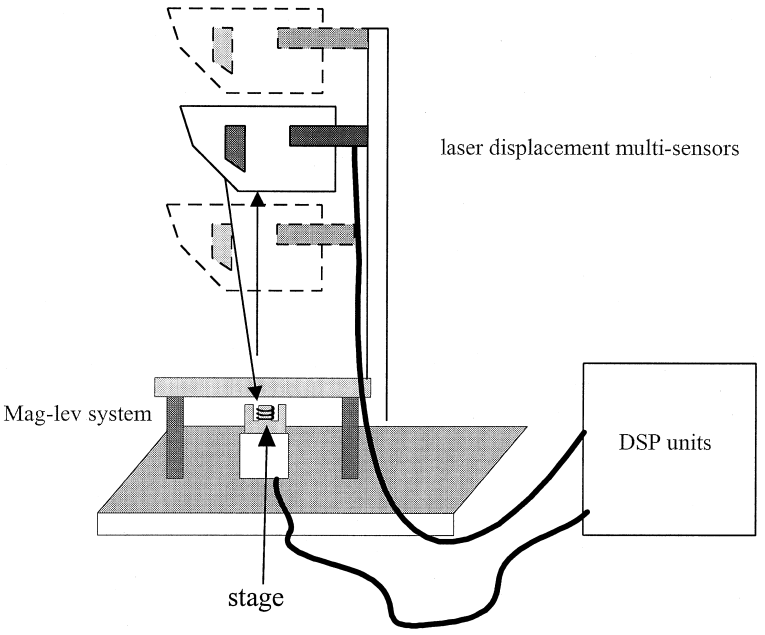


Fig. 1. The set-up of the magnetic levitation and suspension system with laser displacement measurement feedback.

There have been many dissertations on the digital control of magnetic levitation and suspension systems. For example, Trumper et al. [6] designed a linear controller, which provides satisfactory performance, stability, and disturbance rejection over a wide range of operating points. Lin and Gau [7] selected nine output variables to simplify a nonlinear magnetic bearing system into nine linear decoupled subsystems with no internal dynamics using feedback linearization control. Knospe et al. [8] adopted several adaptive on-line synchronous vibration control algorithms demonstrated on a laboratory rotor, supported on magnetic bearings with a high-speed digital controller.

In our system, a special feedback control procedure was developed for a mag-lev control system with multi-information about the displacement. The positioning system framework provides an ideal tool for adaptation and allows the separation of continuous and discrete signals. In this way, it is possible to relate the dynamic behavior of a mag-lev system to a multi-information DSP controlling system. Experiments were performed to test the feasibility of this new control and feedback technique, including calculation of the laser displacement sensors and feedback control of the position of the mag-lev stage.

## 2. Mag-lev system and laser displacement sensor

Fig. 2 depicts the circuit layout of the magnetic levitation system. Using the KVL theorem, the equation for this circuit is produced as follows:

$$V - V_{\text{bias}} = iR' + L(x)\frac{\mathrm{d}i}{\mathrm{d}t} + i\frac{\partial L(x)}{\partial x}\frac{\mathrm{d}x}{\mathrm{d}t}, \tag{1}$$

where $i$ is the current in the coil, $V$ the input voltage, $x$ the length of the air gap, $R'$ the resistance of the emitter and $L(x)$ the inductance of the coil.

In Fig. 3, the E-type core is considered as the combination of two U-type cores. Let $l_A$ be the length of the flux path in the I-type armature and $l_C$ the length of the flux path in the U-type cores. The total impedance of the U-type flux path [9] is determined as follows:

$$R_{U-\text{total}} = R_{\text{core}} + R_{\text{G}} + R_{\text{Armature}} = \frac{l_C + l_A(p/t) + 2\mu_C x}{\mu_0 \mu_C A} = k_1 + k_2 x, \tag{2}$$

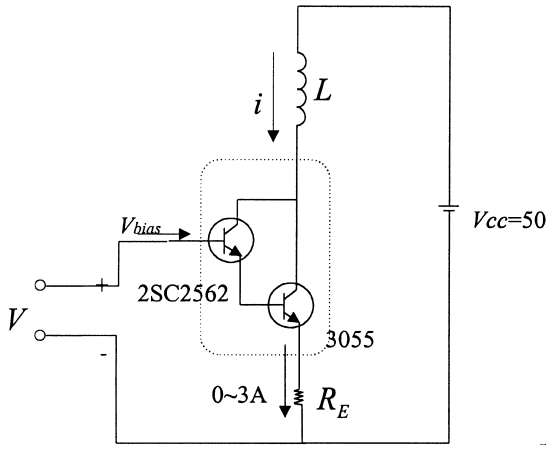


Fig. 2. The layout of control circuit.

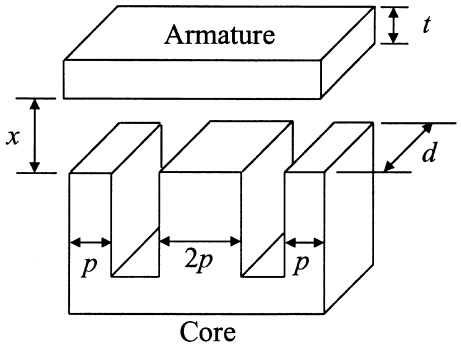


Fig. 3. The structure of the magnetic levitation system.

where

$R_{\text{core}}$ is the impedance of the E-type core, $R_{\text{G}}$ the impedance of the air gap, $R_{\text{Armature}}$ the impedance of the armature. $\mu_{\text{C}}$ the permeability of the E-type core. $\mu_0$ the permeability of the air, $A$ the cross-sectional area.

$$k_1 = \frac{l_C + l_A \frac{p}{t}}{\mu_0 \mu_C A},$$

$$k_2 = \frac{2}{\mu_0 A}.$$

The theory of a laser displacement sensor is based on triangular geometry. It is most linear in the central region, called the standard working distance, falling-off at the sides of the field of view. As shown in Fig. 4, the movement from the standard working point to $A$, $\Delta y$, is proportional to the deviation from the center of the linear optical sensor, $\Delta x$. After modulation an analog output voltage $v_{\text{l}}$ corresponding to the length of the air gap is obtained

$$v_l = K(d - d_0) = K(x - d_{\text{c}}), \tag{3}$$

where, $d$ is the working distance, $d_{\text{f}} < d < d_{\text{n}}$, $d_0$ the standard working distance. $K$ a factor. $d_{\text{f}}$ the far-point of working distance. $d_{\text{n}}$ the near-point of working distance. $d_{\text{c}}$ the compensation distance.

As shown in Fig. 5, the output voltage can be calibrated by zero and span adjustment. Using a set of block gauges $v_l$ can be set to zero when the mag-lev stage is displaced on the standard working distance

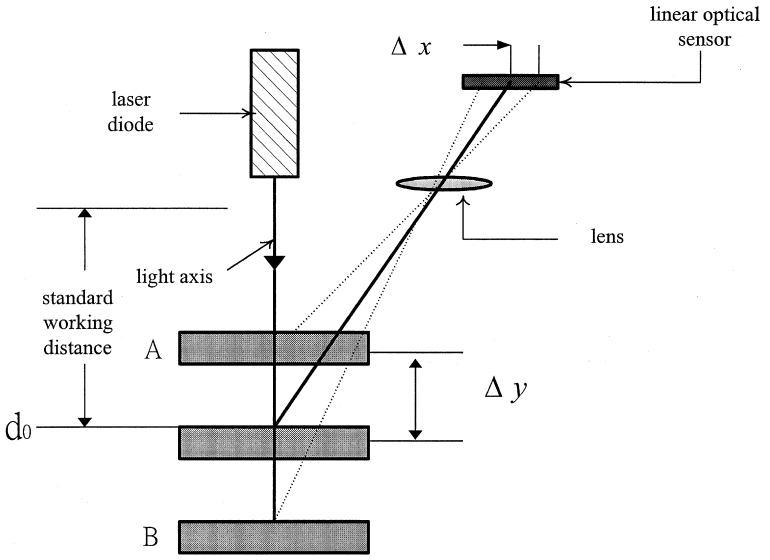


Fig. 4. Conventional triangulation geometry in a laser displacement sensor.

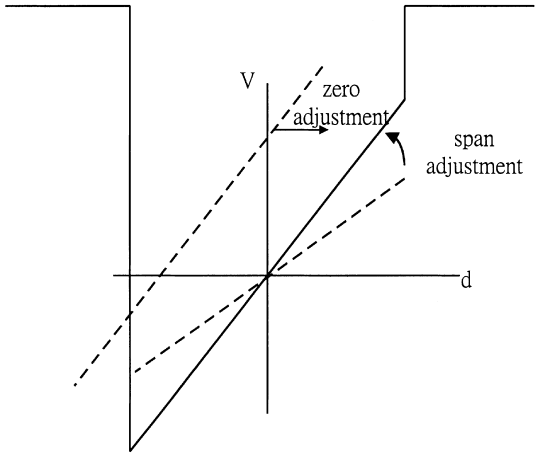


Fig. 5. Zero and span adjustment for a laser displacement sensor.

position. The span adjustment procedures can also confirm that the value of the output voltage is in proportion to the displacement of the mag-lev stage. Then Eqs. (1) and (2) can be re-written as follows:

$$\begin{aligned} V - V_{\text{bias}} &= iR' + L(v_l)\frac{\mathrm{d}i}{\mathrm{d}t} + i\frac{\partial L(v_l)}{\partial x}\frac{\mathrm{d}v_l}{\mathrm{d}t}, \\ R_{U-\text{total}} &= k_1 + k_3(v_l - v_0), \end{aligned} \tag{4}$$

where, $k_3$, $v_0$ are constant.

## 3. System dynamic equation

The path of E-type flux parallels two U-type flux paths, so the total impedance of the E-type flux path $R$ is

$$R = \frac{R_{U-\text{total}} R_{U-\text{total}}}{R_{U-\text{total}} + R_{U-\text{total}}} = \frac{1}{2} R_{U-\text{total}} = \frac{1}{2}(k_1 + k_3(v_l - v_0)). \tag{5}$$

By calculating the impedance, inductance $L(x)$ and air gap $x$ relationship can be determined as follows:

$$L(x) = \frac{n^2}{R} = \frac{2n^2}{k_1 + k_2 x} \quad \text{or} \quad L(v_l) = \frac{n^2}{R} = \frac{2n^2}{k_1 + k_3(v_l - v_0)}, \tag{6}$$

where $n$ is the turn number of the coil. The relationship of the electromagnetic force $F_e$ and the analog output voltage $v_l$ is

$$F_e = -\frac{1}{2} i^2 \frac{dL}{dv_l} = \frac{i^2 n^2 k_2}{(k_1 + k_3 v_l)^2}. \tag{7}$$

From Fig. 6, the equation of motion is as follows:

$$m\ddot{v}_l = mg - F_e = mg - \frac{i^2 n^2 k_3}{(k_1 + k_3 v_l - v_0)^2}, \tag{8}$$

where $m$ is the mass of the E-type core and $g$ is the acceleration of gravity. Let $W_1 = v_l, W_2 = \dot{v}_l, W_3 = i$, the dynamic equation [10] is produced from Eqs. (9)–(11).

$$\dot{W}_1 = W_2, \tag{9}$$

$$\dot{W}_2 = g - \frac{W_3^2 n^2 k_3}{m(k_1 + k_3 W_1)^2}, \tag{10}$$

$$\dot{W}_3 = \frac{\left[R' + \left(\frac{-n^2 k_3}{(k_1 + k_3 W_1)^2}\right) W_2\right](k_1 + k_3 W_1)}{2n^2} W_3 + \left(\frac{k_1 + k_3 W_1}{2n^2}\right)(V - V_{\text{bias}}). \tag{11}$$

By linearizing the dynamic equation and giving the voltage values, current values, and the parameters of the core, a scalar matrix which has $3 \times 3$ dimension and calculate its characteristic equation and its eigenvalues is produced. Therefore, we can determine that the system is stable if all of its poles are in the left-half plane.

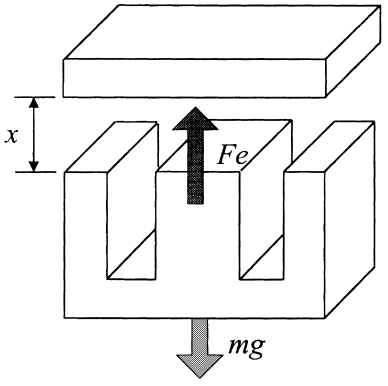


Fig. 6. The forces in the magnetic levitation system.

Table 1
The experimental results of the magnetic levitation and suspension system

| $P$ | $I$ | $D$ | Bias-distance (mm) | Moment behavior | Accuracy |
|---|---|---|---|---|---|
| 5.35 | 5.6e − 5 | 2.3e − 5 | 0.5 | bad | ±10 μm |
| 5.35 | 5.6e − 5 | 2.3e − 5 | 0.4 | bad | ±10 μm |
| 5.35 | 5.6e − 5 | 2.3e − 5 | 0.3 | normal | ±10 μm |
| 5.35 | 5.6e − 5 | 2.3e − 5 | 0.25 | normal | ±5 μm |
| 5.35 | 5.6e − 5 | 2.3e − 5 | 0.2 | normal | ±4 μm |
| 5.35 | 5.6e − 5 | 2.3e − 5 | 0.1 | normal | ±2 μm |
| 5.35 | 5.6e − 5 | 2.3e − 5 | 0.07 | good | ±2 μm |
| 5.35 | 5.6e − 5 | 2.3e − 5 | 0.05 | good | ±2 μm |
| 5.35 | 5.6e − 5 | 2.3e − 5 | 0.03 | excellent | ±1 μm |
| 5.35 | 5.6e − 5 | 2.3e − 5 | 0.02 | excellent | ±1 μm |
| 5.35 | 5.6e − 5 | 2.3e − 5 | 0.015 | good | ±1 μm |
| 5.35 | 5.6e − 5 | 2.3e − 5 | 0.01 | normal | ±1 μm |
| 5.35 | 5.6e − 5 | 2.3e − 5 | 0.005 | normal | ±1 μm |

## 4. The PID control

The parameters of the set-up of laser displacement sensor are: the standard working distance $d_0 = 100$ mm, factor $K = 0.4$ (mV/μm) ,the far-point of working distance $d_f = 114$ mm, the near-point of working distance $d_n = 86$ mm.

To minimize deviation measurements , we must install the laser light perpendicular to the surface of the mag-lev stage. For comparison, the experimental results of PID control of the magnetic levitation and suspension system are shown in Table 1 and Fig. 11.

The rise time, the overshoot, and the steady state error were not good enough. The system was reconfigured with a special feedback control with an auto region selection.

## 5. Auto region selection special feedback control

We refer to Mamdani's mini-operation fuzzy implication [11,12] and adopted the center of area as the defuzzification method. The control mechanism in our system has two input variables, $e(k)$ and $ce(k)$, defined as follows:

$$\begin{aligned} e(k) &= |s - y(k)|, \\ ce(k) &= e(k) - e(k-1), \end{aligned} \tag{12}$$

where $s$ is the set-point, $e(k)$, $e(k-1)$ are the error signals at the time instant $k$ and $k-1$, respectively. The $ce(k)$ is the change of error at time instant $k$. In addition, we defined the input elements, which include the error, change in error, and the output elements.

The three requirements that we considered were: (a) the fast rise time; (b) the smallest overshoot and (c) the smaller steady state error. Intuitively, for a large error $e$, we should set a large $u(k)$. Not only the error $e(k)$, the change in error $ce(k)$ also provides the information of tracking velocity. In our system, we used the strategy that the system would have a larger positive acceleration at the beginning, followed by a reduced rise time and a maximum variation in the incremental control input $u(k)$ to a small value such that the overshoot is reduced or prevented. From our experiment, the structure of the auto region selection positioning controller is shown in Fig. 7. The look up table of the positioning control system is shown in Table 2. The control input $Us(k)$ is calculated as follows:

$$Us(k) = Kr \times u(k), \tag{13}$$

where $Kr$ is the scaling factor.

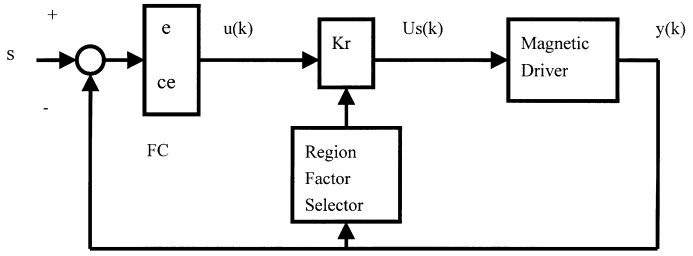


Fig. 7. Auto region selection positioning controller.

Table 2
Look-up table of the positioning control

| $e$ | $u$: $ce$ | | | | | | | | | | |
|---|---|---|---|---|---|---|---|---|---|---|---|
| | −5 | −4 | −3 | −2 | −1 | 0 | 1 | 2 | 3 | 4 | 5 |
| −5 | 4.5 | 4.5 | 4.5 | 4.2 | 3.4 | 2.2 | 1.6 | 1.0 | 0 | 0 | 0 |
| −4 | 4.5 | 4.5 | 4.5 | 4.2 | 3.4 | 2.2 | 1.6 | 1.0 | 0 | 0 | 0 |
| −3 | 4.5 | 4.5 | 4.5 | 4.2 | 3.4 | 2.2 | 1.6 | 1.0 | 0 | 0 | 0 |
| −2 | 4.0 | 4.0 | 4.0 | 3.4 | 2.3 | 1.6 | 1.2 | 0.4 | −0.2 | −0.2 | −0.2 |
| −1 | 3.0 | 3.0 | 3.0 | 2.2 | 2.0 | 1.0 | 0.4 | 0.1 | −0.6 | −0.6 | −0.6 |
| 0 | 0.8 | 0.8 | 0.8 | 0.3 | 0.1 | 0 | −0.1 | −0.6 | −0.9 | −0.9 | −0.9 |
| 1 | 0.3 | 0.3 | 0.3 | −0.2 | −0.3 | −1.0 | −2.0 | −2.1 | −2.8 | −2.8 | −2.8 |
| 2 | 0.1 | 0.1 | 0.1 | −0.5 | −1.1 | −1.5 | −2.5 | −3.1 | −4.1 | −4.1 | −4.1 |
| 3 | 0 | 0 | 0 | −1.0 | −1.5 | −2.1 | −3.2 | −4.2 | −4.5 | −4.5 | −4.5 |
| 4 | 0 | 0 | 0 | −1.0 | −1.5 | −2.1 | −3.2 | −4.2 | −4.5 | −4.5 | −4.5 |
| 5 | 0 | 0 | 0 | −1.0 | −1.5 | −2.1 | −3.2 | −4.2 | −4.5 | −4.5 | −4.5 |

Table 3
The controlled region

| Region | $Kr$ |
|---|---|
| 1 | $0.05d$ |
| 2 | $0.085d$ |
| 3 | $0.015d$ |

The controlled region is divided into the following three regions, where each region depends upon the set-point(s) and the output of magnetic driver $y(k)$ (Table 3):

1. $e(k) < 0.7d$ (positive acceleration region),
2. $0.1d < e(k) \leqslant 0.7d$ (negative acceleration region),
3. $e(k) \leqslant 0.1d$ (stability region),

where

$$e(k) = |s - y(k)|, \quad d = |s - y_0|. \tag{14}$$

In region (1), the present position is very far from the set-point, Therefore, it requires a large control value to turn the output to the set-point quickly, i.e., the output value of the positioning controller must be chosen as large as possible to accelerate the system response. Note that the value of $e(k)$, $ce(k)$ in these region will always be $e(k) > 0$, $ce(k) < 0$. A large scaling factor $Kr$ makes the incremental control input $Us(k)$ large enough to reduce the rise time. The large value of $Us(k)$ will increase the acceleration, so the rise time can be reduced further by increasing the $Us(k)$ value. The value of $e(k)$, $ce(k)$ in region (2) always be $e(k) > 0$, $ce(k) > 0$. The $Us(k)$ value in this region must be limited to prevent an overshoot of the transient response. Thus, the value of the scaling factor $Kr$ is chosen as small as possible for generating a small $Us(k)$

in order to prevent the overshoot. In region (3), the system output is approaching the required position and the set-point is very nearly reached. The oscillation will occur when the value $Us(k)$ is too large or too small, so the scaling factor $Kr$ must be appropriate chose by medium value such that the output approaches the steady state value.

## 6. Experiment

The structure of our mag-lev system consists of a personal computer, a DSP control board, a magnetic driver board, and a main control mechanism. The DSP control board uses a TMS320C50 as the central unit processor and has the ability to perform the complex mathematics calculation. The I/O port of this board has four A/D input and two D/A output channels. The dynamic measurement range of a laser displacement sensor is about 14 mm which is not enough to sense all tracking path (almost 40 mm). Hence, our system cascades three laser displacement sensors to cover the moving path. Each sensor connects with an A/D input channel. After the positioning calculation process, the D/A output channel of the DSP board generates a voltage between 0 and 10 volts to the magnetic driver board that converts 0–3 ampere current for the magnetic driver coil. The detail circuits of the driver board is shown in Fig. 8. The block diagram of the CSDK50 DSP board is shown in Fig. 9.

The special controlling system flow chart is shown in Fig. 10. The operation procedure of the mag-lev system is as follows:

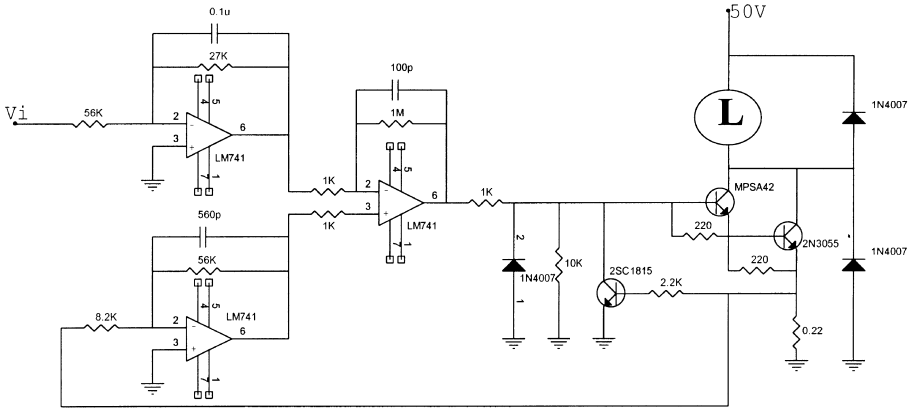


Fig. 8. The detail circuits of the driver board.

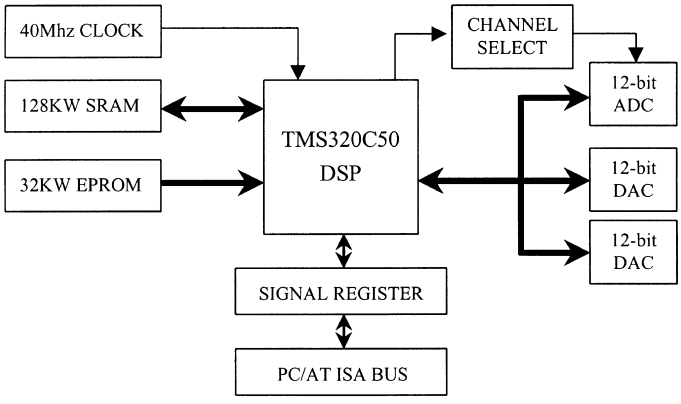


Fig. 9. The function block diagram of CSDK.

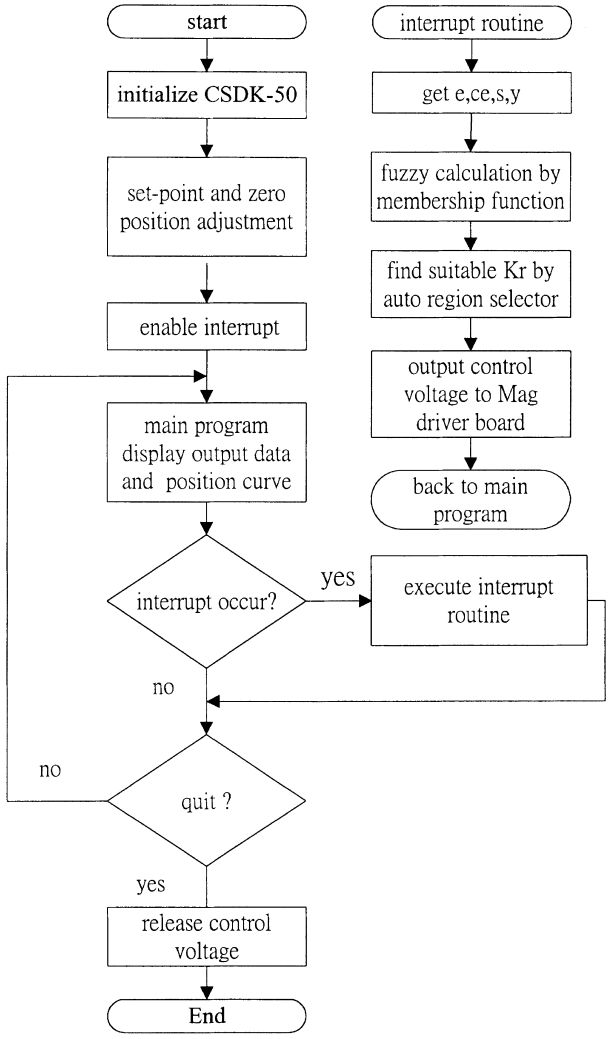


Fig. 10. The system flow chart.

The set-point distance must be entered to the personal computer and the zero position of the system must be adjusted before controlling. The software code should be downloaded to the CSDK50 DSP board that takes charge of the position control during the working time. The laser displacement sensors detect the distance difference between E-type iron core and the vertical moving stage then passes the distance data to

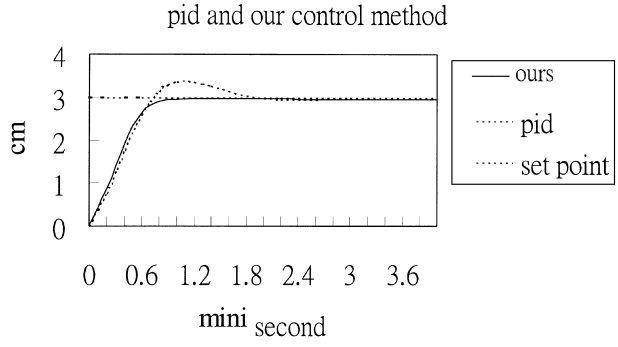


Fig. 11. The experimental results of PID and our positioning control.

the A/D channel of the CSDK50 for advanced decision making calculation. The output signal of the DSP board is the control voltage to be sent out by the D/A channel. The driver board is a voltage to current circuit to convert a suitable driving current to the magnetic coil.

Fig. 11 shows the difference between set-point, PID, and our positioning control. The experiment results show that the positioning control scheme yields a superior transient and steady state performance.

Some problems remain, which are discussed as follows:

(1) Because the resistance in the coil, which on the E-type core does not tend to zero, it is big enough to effect the current in the coil. If the input voltage supplied to the transistor is too large, the transistor will operate in the saturation region. If the input voltage is too small, the current in the coil will become so small that it cannot produce enough electromagnetic force to make the E-type core attract to the I-type armature. Therefore, the regularization of the range of the input voltage becomes an important problem. Therefore, the input voltage of the transistor must be regulated appropriately in the active region, which will create a linear electromagnetic force.

(2) When we designed the OP and DSP circuit, we used a power transistor, which will create a lot of heat. This heat will influence the performance of the devices in the circuit of the system. Therefore, it is important to add a thermo-radiation layer to sponge the heat from the transistor and reduce its heat energy.

## 7. Conclusion

A DSP multi-processor system was built to control a mag-lev stage with a laser displacement sensor feedback. By taking advantage of the laser displacement sensor feedback, a special control method was proposed to reduce the data processing time and increase its accuracy. Experiments on the mag-lev stage position control were performed. The experimental results show a response time shorter than one millisecond and accuracy better than 2 μm.

## Acknowledgements

This work is sponsored by the National Science Council, Taiwan, Republic of China, under grant number NSC 88-2516-S-035-001.

## References

[1] C.S. Lin, R.S. Chang, Fiber optic sensors in the measurement of a vibrating object, J. Precision Eng. 16 (4) (1994) 302–306.
[2] T.C. Strand, Optical three-dimensional sensing for machine vision, Optic. Eng. 24 (1) (1985) 33–40.
[3] C.B. Rao, B. Raj, D.K. Bhattacharya, An optical method for profilometry, Exper. Techniques (1985) 31–34.
[4] United Detector Technology, Electronic Autocollimator Model 1010, 1020, 531 User's Manual (1989) 3–20.
[5] E.G. Loewen, High speed optical scanning techniques for dimensional measurement, Ann. CIRP 29 (2) (1980) 513–518.
[6] D.L. Trumper, S.M. Olson, P.K. Subrahmanyan, Linearizing control of magnetic suspension systems, IEEE Trans. Control Syst. Technol. 5 (4) (1997) 427–438.
[7] L.C. Lin, T.B. Gau, Feedback linearization and fuzzy control for conical magnetic bearings, IEEE Trans. Control Syst. Technol. 5 (4) (1997) 417–426.
[8] C.R. Knospe, S.J. Fedigan, R.W. Hope, R.D. Williams, A multitasking dsp implementation of adaptive magnetic bearing control, IEEE Trans. Control Syst. Technol. 5 (2) (1997) 230–238.
[9] P.C. Sen, Principle of Electric Machines and Power Electronics, Wiley, New York, 1989, pp. 101–123 (Chapter 3).
[10] M.S. Sarma, Electric Machines, West Publishing, 1994, 507–24 (Chapter 11).
[11] E.H. Mamdani, Applications of fuzzy algorithms for control simple dynamic plant, in: Proceeding of the IEEE, 121 December 1974, pp. 1585–1588.
[12] C.C. Wong, S.M. Feng, Switching-Type Fuzzy Controller Design,1994 Second National Conference on Fuzzy and Applications (1994) 7–12.